

An Experimental Investigation of EOR Mechanisms for Nanoparticles Fluid in Glass Micromodel

Shidong Li and Ole Torsæter,

Norwegian University of Science and Technology (NTNU)

This paper was prepared for presentation at the International Symposium of the Society of Core Analysts held in Avignon, France, 8-11 September, 2014

ABSTRACT

Nanoparticle as part of nanotechnology has already drawn attentions for its great potential of enhancing oil recovery. In the last few years some publications have already addressed this topic, but the basic enhanced oil recovery (EOR) mechanisms have not been released very clearly. In this experimental study a visualization flooding method (glass micromodel) was used to investigate the EOR mechanisms of nanoparticles fluid.

In this experimental study both silica nano-structured particle and colloidal silica nanoparticle were used to enhance oil recovery. A transparent glass micromodel was utilized as porous media, and synthetic brine was used to disperse nanoparticles. The effects of different kinds of nanoparticles and different nanoparticle concentrations on EOR were investigated; and some properties between oil and water were measured to uncover EOR mechanisms. The experimental results showed that nanoparticles have the ability to reduce the IFT between oil and water as well as contact angle, to make solid surface to be more water wet. In the visualization flooding experiments, as the nanoparticles concentration increase more trapped oil can be produced by emulsification and reduction of IFT. Pore channels plugged due to adsorption of nanoparticles were observed and resulted in increase of injection pressure, which pushed some trapped oil in the small pore channels out of the model. The results from the glass micromodel study give a clear indication that the EOR potential of nanoparticles fluid is significant.

INTRODUCTION

As a part of nanotechnology, nanoparticles fluid was proposed as a new method to meet the huge oil demand in the future. Nanoparticles are generally defined as particles with size ranges from 1nm-100nm and the nanoparticle fluid is defined as dispersion (suspension) of nanoparticles in various fluids. Nanotechnology emerged in the 1980s and has already been utilized successfully in many industries. As reported by Kong et al. (2010) [1] and Kapusta et al. (2012) [2], nanotechnology has the potential to be used in many disciplines of oil and gas industry. The particle size of nanoparticle is much smaller than conventional reservoir rock pore channel, so that nanoparticles can penetrate through reservoir easily. Based on many publications, it has been suggested that silica nanoparticle fluids have the potential for EOR. [3, 4], moreover Ogolo et al. (2012) [5] and Hendraningrat et al. (2014) [6] have discussed the possibility of using metal oxides nanoparticles, including oxides of aluminum, zinc, magnesium, zirconium, titanium.

The nanoparticles used in this experiment are hydrophilic silica nanoparticle. Silica nanoparticle has many advantages as EOR agent, for instance, 1) 99.8% of silica nanoparticle is silicon dioxide (SiO_2), which is main component of sandstone, so silica nanoparticle is an environmentally friendly material compared to chemical substance; 2) since the silica nanoparticle is made from silicon dioxide, so the raw material (quartz) is easy to be obtained, and the price is cheaper than chemical, this makes silica nanoparticle applicable for EOR in oil field; 3) the chemical behavior of the nanoparticle can be controlled by changing the composition of the surface coating, for example nanoparticle can be changed from hydrophilic to hydrophobic by adding lipophilic group.

The EOR mechanisms for nanofluid have already been discussed in several publications [7, 8], which include disjoining pressure, interfacial tension (IFT) reduction, wettability alteration and pore channels plugging. The hydrophilic nanoparticle suspension was found has capability to reduce IFT and contact angle between oil and water. In this paper the work was focused on investigate the EOR mechanisms for both silica nano-structured particle and colloidal silica nanoparticle by using visualization flooding method.

EXPERIMENTAL MATERIALS AND METHODS

Experimental Material

1. Nanoparticle: Both nano-structured particle (NSP) and colloidal nanoparticle (CNP) were applied in experiments. NSP has primary particle size 7 nm, after been dispersed in 3 wt. % brine, particles might aggregate to form bigger particle. CNP has particle size about 8 nm, and it is suspension fluid of nanoparticles with stabilizer. They are produced by Evonik Industries and their specific surface area is around $300\text{m}^2/\text{g}$ and $350\text{m}^2/\text{g}$ respectively. The nanoparticles have been characterized under Scanning Electron Microscope (SEM), and the pictures are shown in **Figure 1**.

2. Nanofluids: The nanofluids with various weight concentrations (0.05, 0.1 and 0.5 wt. %) were prepared by sonicator and 3 wt. % brine was used as dispersion fluid for hydrophilic nanoparticle, the density and viscosity of nanofluids are similar to water. 0.5 wt. % concentration case not used for NSP fluid due to the unfavorable stability of nanoparticles fluid.

3. Oil: The oil used in this experiment is crude oil from North Sea, the density is $0.84\text{g}/\text{ml}$ and viscosity is 18.4 cP.

4. Porous media: A transparent glass micromodel was utilized in the visualization flooding experiments. The glass micromodel is made of a two-dimensional pore structure etched onto the surface of a flat glass plate, which is covered by another glass plate, thus creating an enclosed pore space [9]. Pore structure and parameter of glass micromodel were shown in **Figure 2** and **Table 1**.

5. Flooding setup: **Figure 3** shows schematic of flooding setup. The pump injected Exxol D-60 as pumping fluid to push the piston located inside the cylinder containers. There are 3 cylinder containers filled with brine, crude oil and nanofluid above the piston respectively. The hosting system and imaging capturing system (optical microscope,

video camera, computer and software) were used to capture image for glass micromodel. The pressure drop of glass micromodel during flooding experiments was recorded by precision pressure gauge.

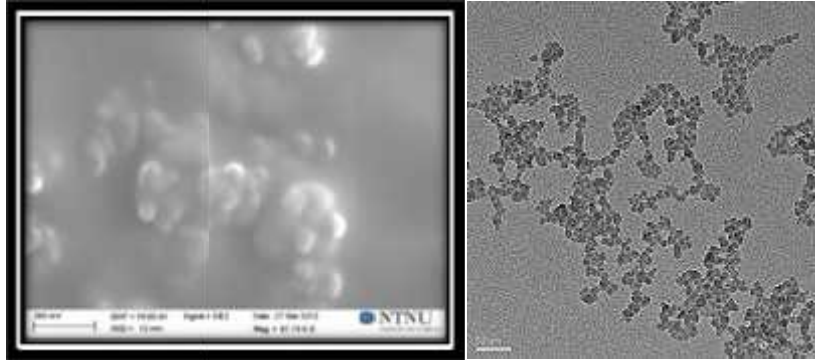


Figure 1 SEM image for nanoparticles (left: nano-structured particle; right: colloidal nanoparticle from Evonik)

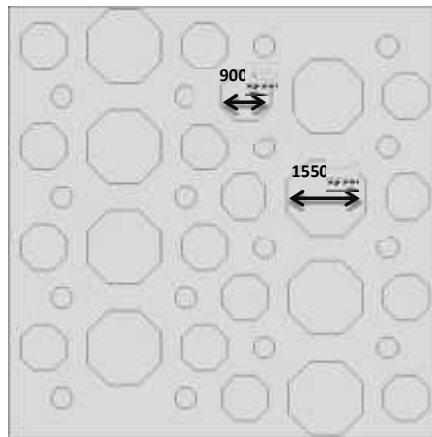
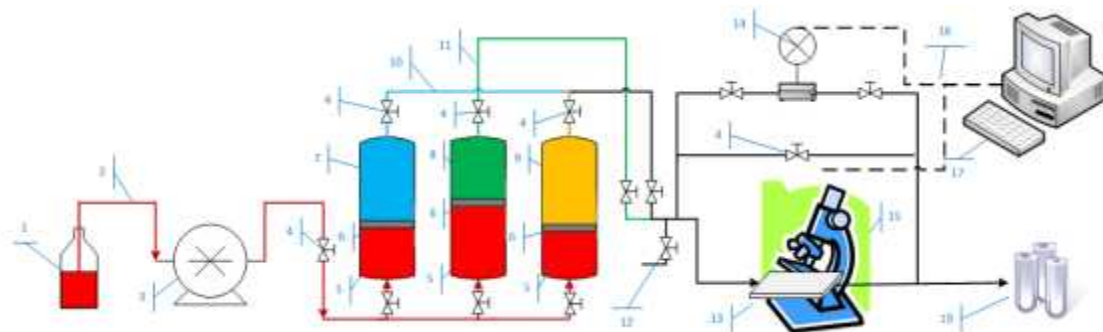


Figure 2 Porous structure of glass micromodel



- 1) Pump fluid (Exxol D60); 2) injection line; 3) Micro Pump; 4) Valve; 5) Cylinder container; 6) Piston plate; 7) Brine in container; 8) Oil in container; 9) Nanofluid in container; 10) Brine/Nanofluid line; 11) Oil line; 12) Bypass Valve; 13) Glass micromodel; 14) Pressure gauge; 15) Microscope 16) connection cable; 17) Computer; 18) Accumulator tubes

Figure 3 Schematic of flooding setup

Table 1 Glass Micromodel characteristics

Parameter	Micromodel
Length (cm)	7.4
Width (cm)	4
Depth (cm)	0.01
Porosity (%)	0.44
PV (ml)	0.13
Typical channel width (μm)	400-550
Permeability (Darcy)	about 5

Experimental Methods

1. Interfacial tension measurement

The IFT between crude oil and brine/nanofluids was measured by using SVT20 spinning drop tension meter at ambient condition. The drop volume was in range 1-3 μL . The rotation speed was kept around 4000-6000 rpm. In the result of centrifugal field, the drop elongates along the axis of rotation. The interfacial tension opposes the elongation because of the increase in area and a configuration which minimizes system free energy is reached [10].

2. Contact angle measurement

In this experiment, contact angle between crude oil and brine/nanofluids was measured by using Goniometry KSV CAM instrument at room condition. Polished quartz was used as solid surface, and a small droplet of crude oil was laid under the quartz surface, which was immersed inside the brine or nanofluid. The measurement was run enough time until system reach equilibrium.

3. Visualization flooding experiments

Before each visualization flooding experiment, the glass micromodel was cleaned by toluene and methanol. For two-phase flooding experiments, firstly the glass micromodel was fully saturated with brine, and then crude oil was injected into the micromodel with injection rate of 0.2ml/min to displace brine, so the initial water saturation was established. For the first imbibition process, brine was injected at constant injection rate of 0.02 ml /min until no more oil was produced, and then injection rate was increased to 0.04 ml/min to see if more oil could be displaced. Then different concentrations nanofluids were injected with injection rate 0.02 ml/min and 0.04 ml/min to investigate the effect of nanofluids on EOR. Water-oil distribution images of interesting areas were taken to evaluate the results.

RESULTS AND DISCUSSION

Effect of concentration of nanofluids on IFT

Introducing of hydrophilic silica nanoparticles into the brine-oil system was observed to reduce IFT and have potential to release some residual oil trapped by capillary pressure. The mechanism for reduction of IFT might be the hydrophilic part of nanoparticles tends to be present in the aqueous phase and the hydrophobic part like to exist in the oil phase,

so nanoparticles can adsorb on the interface between oil and water to replace the previous one, the friction force of those two phases reduce and thereby generate lower IFT.

Figure 4 shows that IFT decreases with increase of nanoparticle concentration for both CNP and NSP. But at the same concentration CNP fluid has lower IFT than NSP within 0.1 wt. % nanoparticle concentration, so CNP has better capability to reduce IFT than NSP.

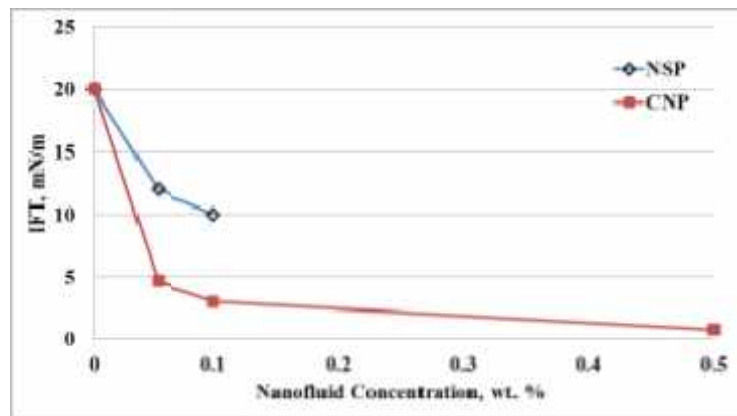


Figure 4 IFT between oil and NSP/CNP fluids with different concentration

Effect of concentration of nanofluids on contact angle

Due to the large specific surface area of nanoparticle, it can easily adsorb on solid surface, so that the original wettability could be changed. Since both CNP and NSP are hydrophilic nanoparticles, so adsorption of nanoparticle on glass plate can make surface to be more water wet. **Figure 5** shows contact angle measurements of crude oil against brine/nanofluids at various concentrations. CNP and NSP have ability to reduce the contact angle between oil and water, and contact angle decline when concentration increase. For the same concentration, CNP can make surface more water wet than NSB. Due to very low IFT between 0.5 wt. % CNP fluid and oil, contact angle measure couldn't be conducted.

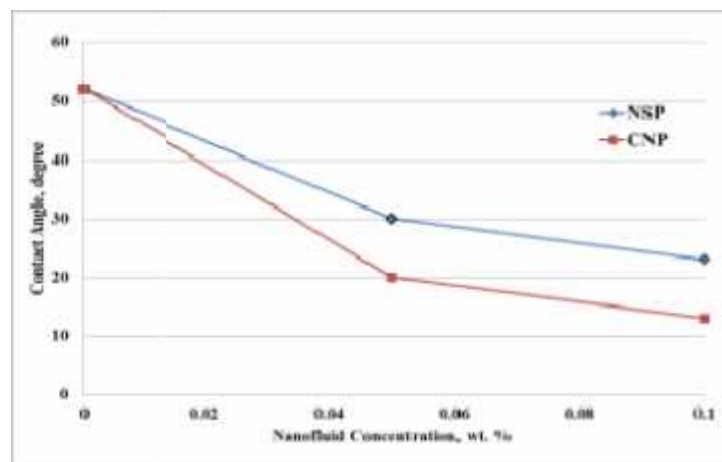


Figure 5 Contact angle between oil and NSP/CNP fluids with different concentration

Visualization flooding experiments

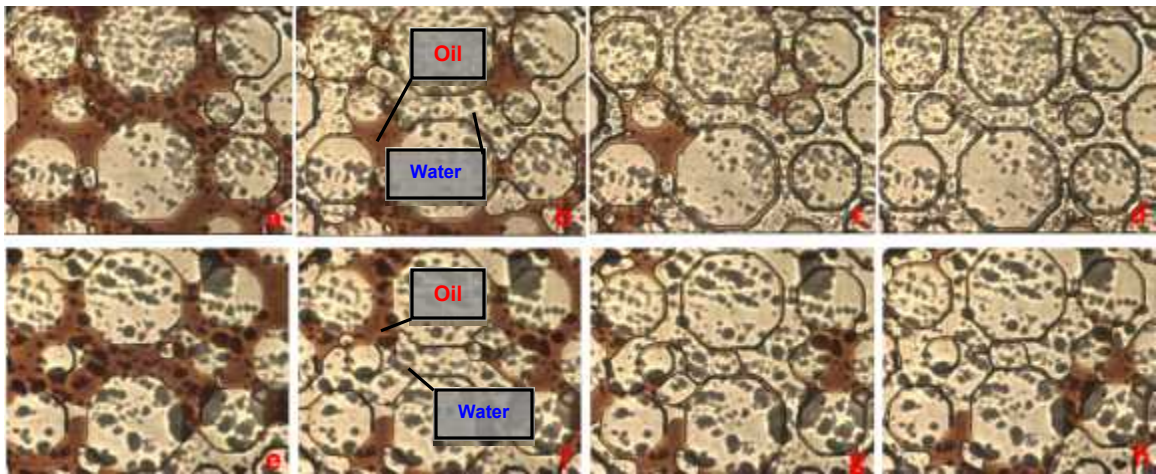
The flooding experiments of glass micromodel make it possible to observe the microscopic behavior of oil and aqueous phases in porous media. This is a significant advantage to study the displacement of two immiscible fluids, and this method makes it easier to investigate EOR mechanism, especially for a new EOR method.

Effect of CNP and NSP fluids on EOR

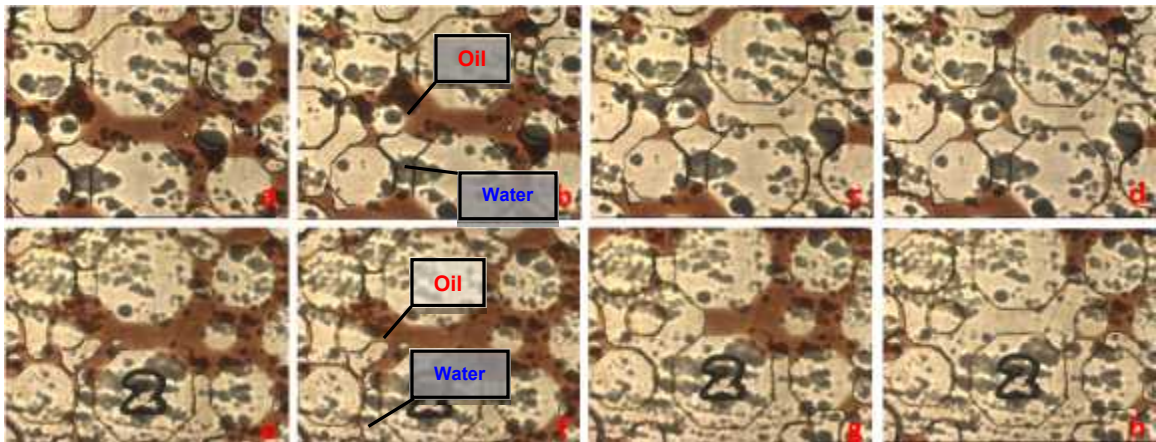
Three different concentrations (0.05 wt. %, 0.1 wt. % and 0.5 wt. %) of CNP fluids and two different concentrations (0.05 wt. % and 0.1 wt. %) of NSP fluids were used as tertiary recovery agent in visualization flooding experiments, flooding scenario was mentioned before. Some interesting areas were selected to evaluate effect of nanoparticle fluids on EOR and analyze EOR mechanisms. The oil saturation pictures of whole glass micromodel were also taken to assist in uncovering unknown mechanisms. Since the pore volume of glass micromodel is only 0.13ml, it's very difficult to quantify the recovery, image analyzing can be a good way to discuss results qualitatively.

The results of different concentration CNP fluids are shown in **Figure 6-9**, from microscope images of micromodel, both increase of injection rate and injection of nanofluids have ability to produce more residual oil, but injection rate has only limit effect on EOR, similar results also can be got from glass micromodel oil saturation image (**Figure 11-13**). However, as we can see in **Figure 6-9**, after injection of CNP fluids pore volume occupied by oil decreased significantly compared with water flooding, even though with low concentration and low injection rate. While the medium and high concentration cases (**Figure 12, 13**) have better EOR effect than low concentration case (**Figure 11**). For low and medium concentration cases (0.05 wt. % and 0.1 wt. %) when injection rate increased to 0.04 ml/min, some residual oil also can be pushed out, while for high concentration case (0.5 wt. %) increase of injection rate had no significant effect on EOR, since IFT of 0.5 wt. % is quite low most of oil can be produced out under 0.02 ml/min injection. From above experimental results it can be concluded that the main EOR mechanisms of CNP fluid might be IFT reduction as well as emulsification for high CNP concentration fluid (0.5 wt. %).

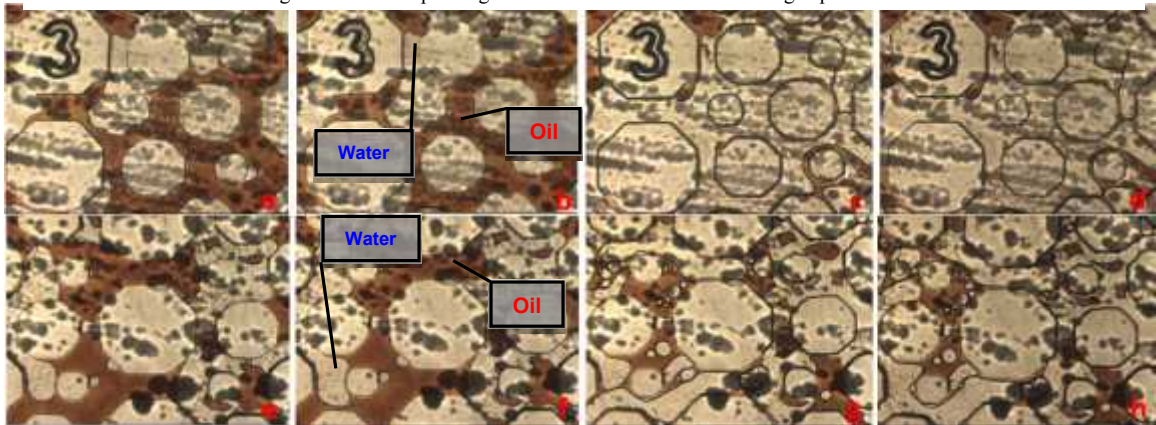
As we can see in **Figure 9, 10**, for imbibition process when injection rate of brine increased, some oil were produced. After NSP fluids were injected, the amount of oil drop also decreased and continued to decline when the injection rate increased for all experiments. However, for low concentration nanofluid cases, there is no significant reduction of oil drops for water flooding and nanofluid injection with 0.02 ml/min, but oil saturation reduced somehow when injection rate increased to 0.04 ml/min. So we can conclude that for low concentration nanofluid flooding, concentration of nanofluid is not an important factor for recovery, it is still dominated by injection rate. While for higher concentration case oil saturation decreased and oil drops restarted moving when nanofluids are injected into the model, and some big oil drops broke to small oil drops (emulsion) when injection rate increased, which is helpful for oil drops to go through the small pore channels to reduce the effect of capillary pressure.



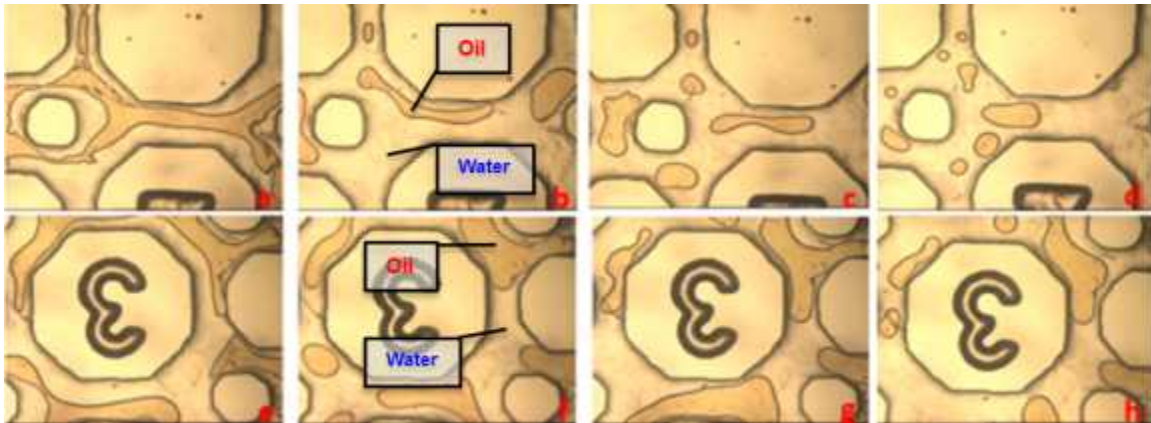
a and e: Brine flooding (BF) 0.02ml/min; b and f: BF 0.04ml/min; c and g: nanofluid flooding (NF) 0.02ml/min; d and h: NF 0.04 ml/min
 Figure 6 Microscope image for 0.05 wt. % CNP fluids flooding experiments



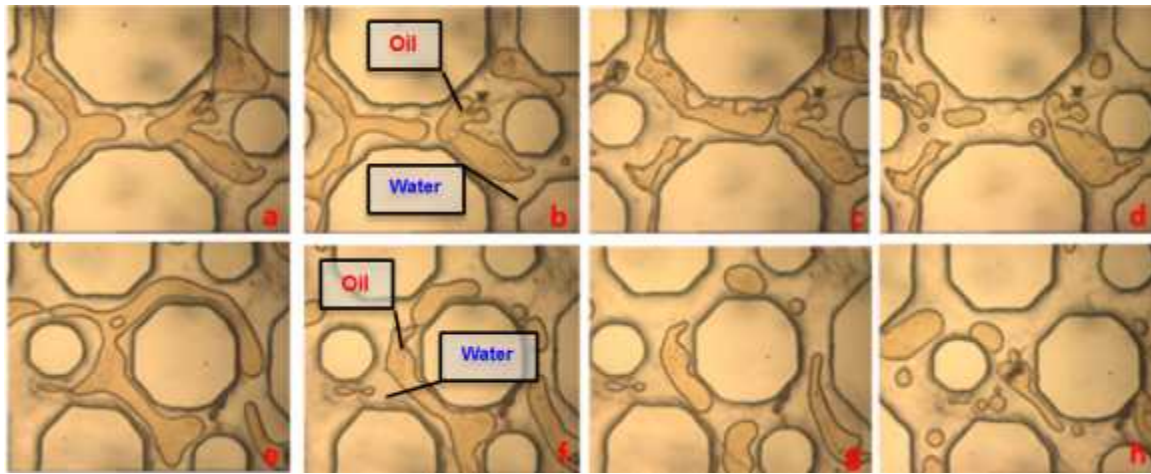
a and e: Brine flooding (BF) 0.02ml/min; b and f: BF 0.04ml/min; c and g: nanofluid flooding (NF) 0.02ml/min; d and h: NF 0.04 ml/min
 Figure 7 Microscope image for 0.1 wt. % CNP fluids flooding experiments



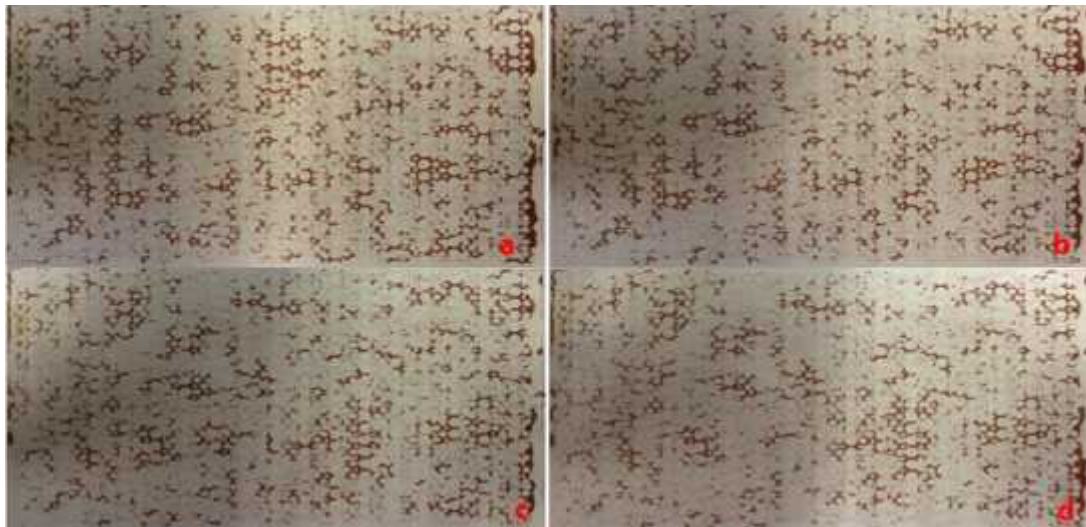
a and e: Brine flooding (BF) 0.02ml/min; b and f: BF 0.04ml/min; c and g: nanofluid flooding (NF) 0.02ml/min; d and h: NF 0.04 ml/min
 Figure 8 Microscope image for 0.5 wt. % CNP fluids flooding experiments



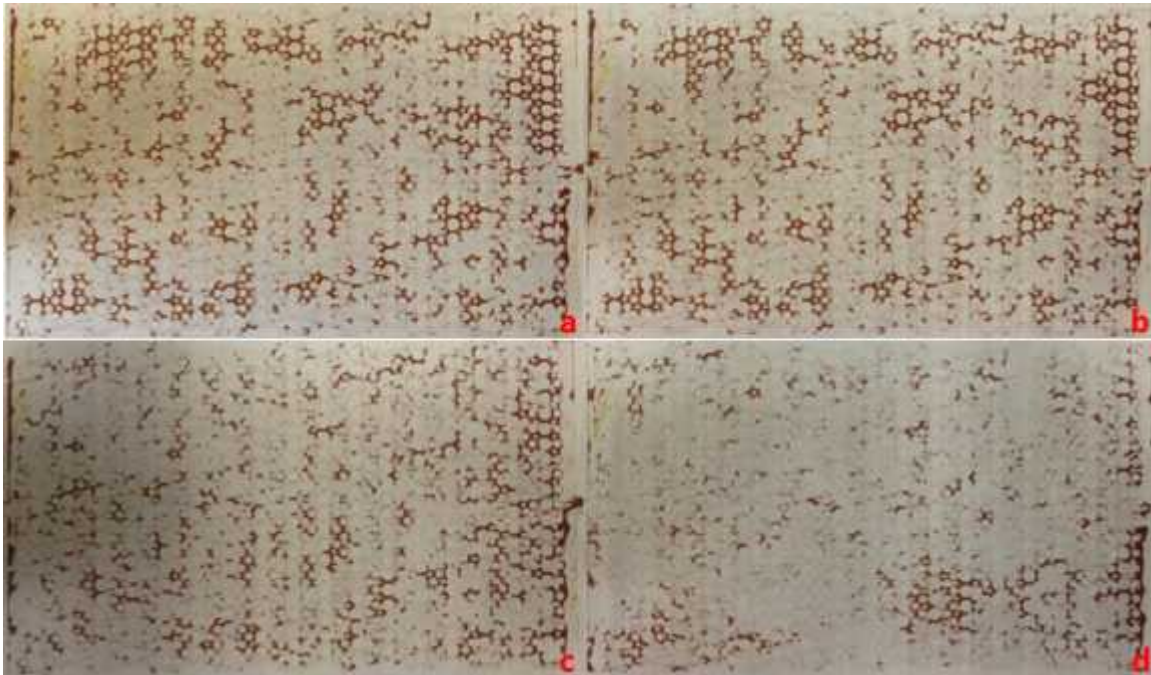
a and e: Brine flooding (BF) 0.02ml/min; b and f: BF 0.04ml/min; c and g: nanofluid flooding (NF) 0.02ml/min; d and h: NF 0.04 ml/min
 Figure 9 Microscope image for 0.05 wt. % NSP fluids flooding experiments



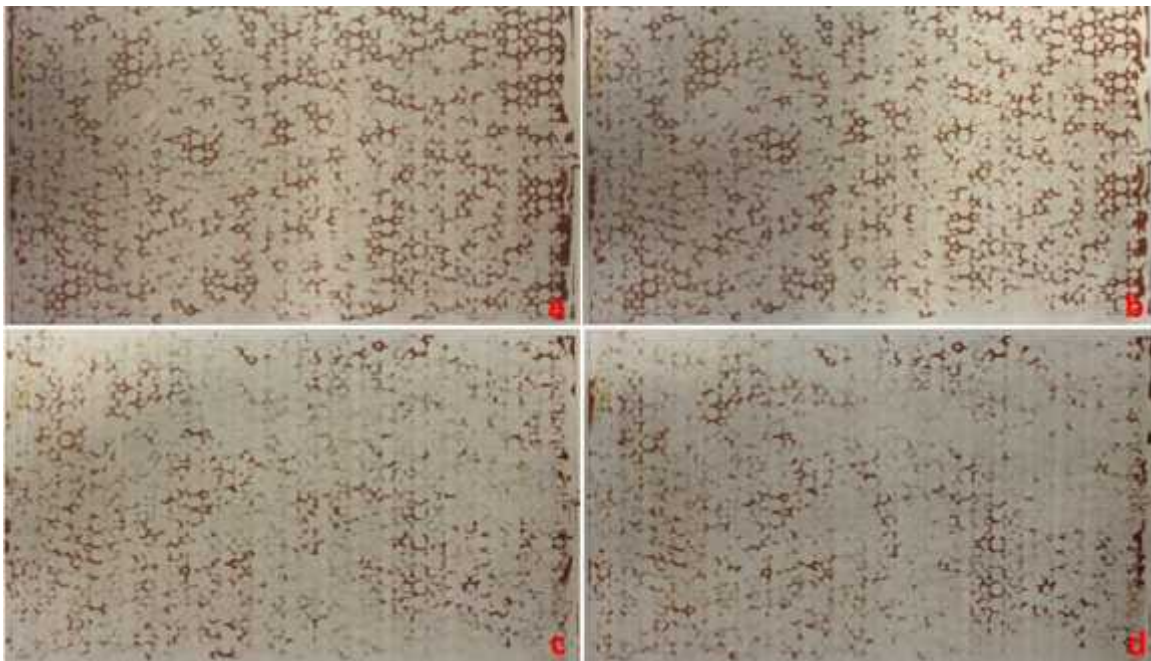
a and e: Brine flooding (BF) 0.02ml/min; b and f: BF 0.04ml/min; c and g: nanofluid flooding (NF) 0.02ml/min; d and h: NF 0.04 ml/min
 Figure 10 Microscope image for 0.1 wt. % NSP fluids flooding experiments



a: Brine flooding (BF) 0.02ml/min; b: BF 0.04ml/min; c: nanofluid flooding (NF) 0.02ml/min; d: NF 0.04 ml/min
 Figure 11 Glass micromodel oil saturation image for 0.05 wt. % CNP fluids flooding experiments



a : Brine flooding (BF) 0.02ml/min; b: BF 0.04ml/min; c: nanofluid flooding (NF) 0.02ml/min; d: NF 0.04 ml/min
Figure 12 Glass micromodel oil saturation image for 0.1 wt. % CNP fluids flooding experiments



a : Brine flooding (BF) 0.02ml/min; b: BF 0.04ml/min; c: nanofluid flooding (NF) 0.02ml/min; d: NF 0.04 ml/min
Figure 13 Glass micromodel oil saturation image for 0.5 wt. % CNP fluids flooding experiments

Adsorption of nanoparticles and plugging inside glass micromodel

Since nanoparticle has huge specific surface area, they adsorb easily in porous media, the images for adsorption of nanoparticle in glass micromodel were presented in previous authors' paper [7]. Adsorption of nanoparticle in glass micromodel might result in

plugging of pore channels and reduction of permeability, in order to investigate effect of adsorption pressure drop data were recorded during flooding experiments. As shown in **Figure 14**, for CNP fluid case during nanofluid flooding pressure drop can quickly reach a low value and stay constant until oil saturation reaches equilibrium state. However, in NSP fluid flooding experiments pressure drop increased continuously and until it reached the limit of the pressure gauge. The results indicate that NSP is much easier to adsorb inside micromodel than CNP and lead to the permeability reduction.

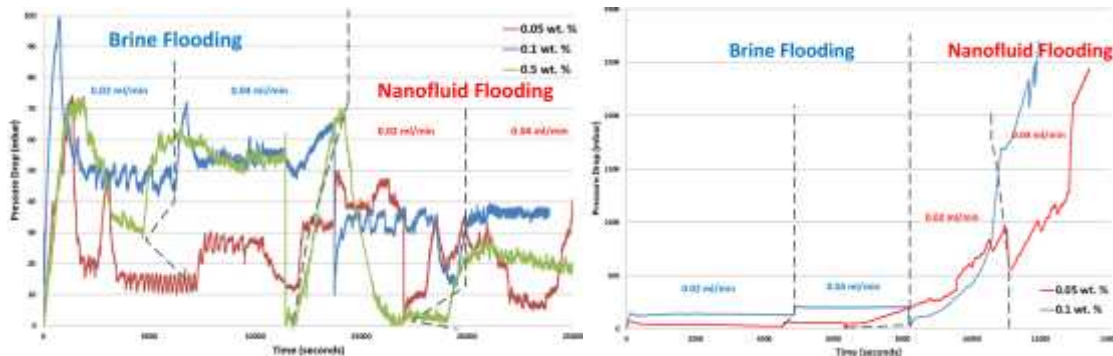


Figure 14 Pressure drop of glass micromodel flooding experiments (left:CNP fluid; right:NSP fluid)

Flow pattern change with nanoparticle

Two glass micromodel oil saturation images were taken at brine breakthrough time to see flow pattern change due to CNP injection. As shown in **Figure 15**, before injection of CNP fluids the first breakthrough channel located at top of micromodel, shown with red arrow, but after injection of nanoparticles the first breakthrough channels were shifted to middle and bottom of the model, which means volumetric sweep efficiency increased and more oil can be produced out. The possible reason might be pore channels plugging and wettability alteration.

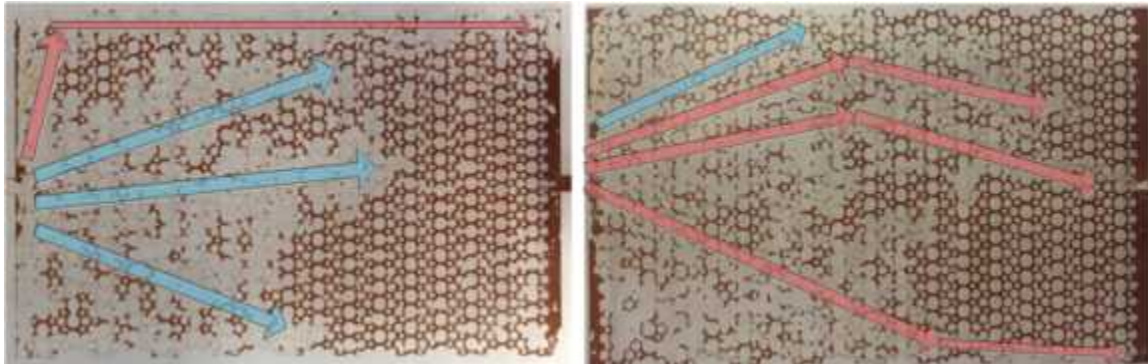


Figure 15 Glass micromodel oil saturation image at brine breakthrough time (left: before CNP injection; right after CNP injection. Red arrow: first breakthrough path; blue arrow: late breakthrough path)

Emulsion stabilized by nanoparticles

As reported by Zhang et al. (2010) [11], nanoparticle can stabilize emulsions. Theoretically hydrophilic nanoparticles stabilize oil-in-water (o/w) emulsion and hydrophobic nanoparticles can stabilize water-in-oil (w/o) emulsion. Both NSP and CNP

that used in this paper are hydrophilic nanoparticle, and as shown in **Figure 16**, o/w emulsions were observed in NSP fluid flooding experiments with 0.5 wt. % and 0.04 ml/min flow rate, while for CNP fluid flooding experiments with 0.5 wt. % and 0.04 ml/min flow rate w/o emulsions were observed, which is a strange phenomenon, the reason is still unknown. And this emulsification only happened in high concentration flooding experiments, while for low concentration cases if injection rate is high enough emulsions stabilized by nanoparticles also were observed.

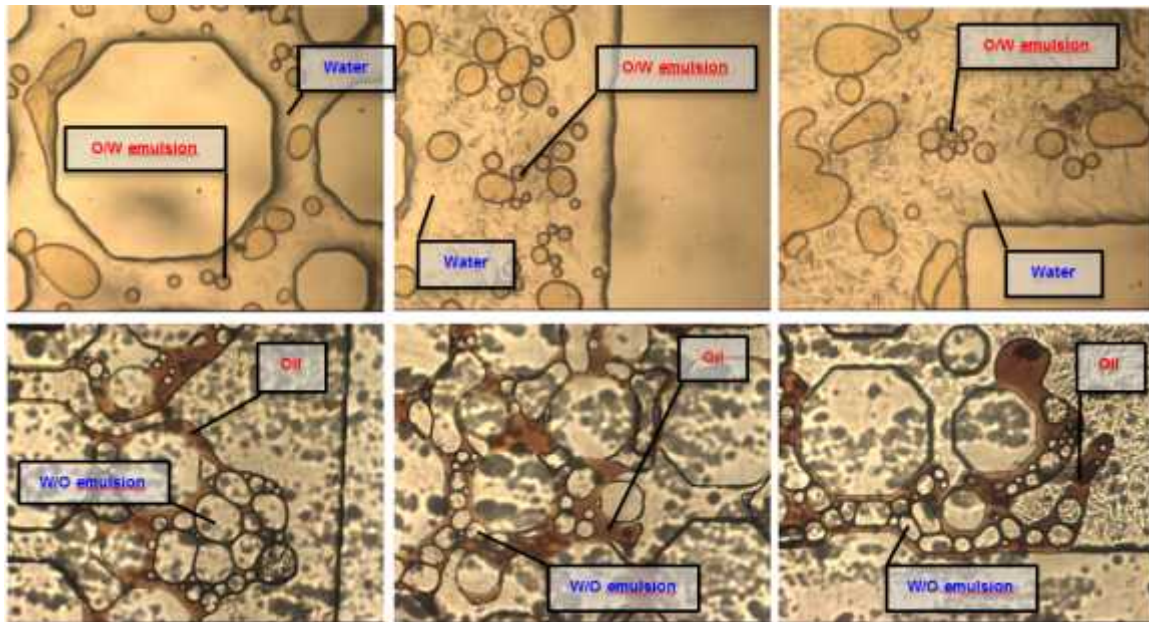


Figure 16 Emulsions stabilized by nanoparticles (up three: O/W emulsion stabilized by NSP; bottom three W/O emulsion stabilized by CNP)

CONCLUSIONS

1. Both for NSP and CNP have ability to reduce IFT, and IFT decrease when nanoparticle concentration increase. At the same concentration of nanoparticles NSP can reduce more IFT than CNP.
2. Contact angle between water and oil was decrease when introducing NSP and CNP, and contact angle decline when concentration of nanoparticle increases. For the same concentration CNP can make surface more water wet than NSP.
3. For visualization flooding experiments, both NSP and CNP can increase oil recovery and when nanoparticle concentration increase more additional oil can be produced. The EOR mechanisms for CNP include IFT reduction and emulsification (water in oil emulsion), NSP fluid's EOR mechanisms are IFT reduction and breaking oil into small oil drop (oil in water emulsion).
4. NSP has better adsorption ability in porous media than CNP, so injection of NSP can reduce the permeability of micromodel and increase injection pressure during flooding.

5. Injection of CNP fluids can change flow pattern, and the first breakthrough channel can be shifted to others, so that volumetric sweep efficiency increase.

6 CNP can stabilize water in oil emulsion at high flow rate or high concentration, while oil in water emulsion can be stabilized by NSP at the same condition.

REFERENCES

1. Kong, X., Ohadi, M. M. Applications of Micro and Nano Technologies in the Oil and Gas Industry- An Overview of the Recent Progress. SPE-138241(2010).
2. Kapusta, S., Balzano, L., Riele, P. Nanotechnology Application in Oil and Gas Exploration and Production. IPTC-15152 (2012).
3. Skauge, T., Spildo, K., Skauge, A. Nano-sized Particles for EOR. SPE 129933-MS(2010).
4. Hendraningrat, L., Li, S., Torsæter, O. A Coreflood Investigation of Nanofluid Enhanced Oil Recovery in Low-Medium Permeability Berea Sandstone. SPE 164106-MS (2013).
5. Ogolo, N. A., Olafuyi, O. A., Onyekonwu, M. O. Enhanced Oil Recovery Using Nanoparticles. Paper SPE 160847 (2012).
6. Hendraningrat, L., Torsæter, O. Unlocking the Potential of Metal Oxides Nanoparticles to Enhance the Oil Recovery. OTC-24696-MS (2014).
7. Li, S., Hendraningrat, L., Torsæter, O. Improved Oil Recovery by Hydrophilic Silica Nanoparticles Suspension: 2-Phase Flow Experimental Studies. IPTC-16707-MS (2013).
8. Suleimanov, B.A., Ismailov, F.S., Veliyev, E.F. Nanofluid for enhanced oil recovery. Journal of Petroleum Science and Engineering, (2011) Volume 78, Issue 2, Pages 431–437.
9. Afrapoli, M.S., 2010. Experimental Study of Displacement Mechanism in Microbial Improved Oil Recovery. Doctoral Thesis at Department of Petroleum Engineering and Applied Geophysics, Norwegian University of Science and Technology (NTNU). Trondheim, Norway.
10. Torsæter, O., Abtahi, M. Experimental Reservoir Engineering Laboratory Workbook, (2003).
11. Zhang, T., Davidson, D., Bryant, S. L., Huh, C. Nanoparticle-Stabilized Emulsions for Applications in Enhanced Oil Recovery. SPE-129885-MS (2010) .